Molecular Crystals and Liquid Crystals

ISSN: 1542-1406 (Print) 1563-5287 (Online) Journal homepage: http://www.tandfonline.com/loi/gmcl20

Nanostructured lipid carriers with liquid crystal structure encapsulating phenylethyl resorcinol: Characterization and in vitro study

F. Jia, H. Gao, H. Jia & W. Zhang

To cite this article: F. Jia, H. Gao, H. Jia & W. Zhang (2016) Nanostructured lipid carriers with liquid crystal structure encapsulating phenylethyl resorcinol: Characterization and in vitro study, Molecular Crystals and Liquid Crystals, 633:1, 1-13, DOI: 10.1080/15421406.2016.1177873

To link to this article: http://dx.doi.org/10.1080/15421406.2016.1177873

MOLECULAR CRYSTALS AND LIQUID CRYSTALS
2016, VOL. 633, 1–13
http://dx.doi.org/10.1080/15421406.2016.1177873

Taylor & Francis
Taylor & Francis Group

Nanostructured lipid carriers with liquid crystal structure encapsulating phenylethyl resorcinol: Characterization and *in vitro* study

F. Jia[a], H. Gao[b], H. Jia[a], and W. Zhang[a]

[a]School of Perfume and Aroma Technology, Shanghai Institute of Technology, Fengxian district, Shanghai, China; [b]Electron Microscpy Core Laboratory, Shanghai Medical College, Fudan University, Xuhui district, Shanghai, China

ABSTRACT

A new nanocarrier encapsulation technology that combined the advantages of liquid crystal (LC) and nanostructured lipid carriers was developed to overcome the problems related to the presence of phenylethyl resorcinol (PR) in cosmetic products. This paper described the characterization and in vitro evaluation of nanostructured lipid carriers (NLC) with an LC structure encapsulating PR (PR–LC–NLC). It demonstrated a spherical morphology, high drug entrapment efficiency, and excellent long-term stability. A prolonged release profile of PR from PR–LC–NLC was obtained. And it increased the PR's skin retention in the in vitro penetration study.

KEYWORDS

nanostructured lipid carriers; liquid crystal; Phenylethyl resorcinol; in vitro drug release; in vitro penetration

1. Introduction

Skin whitening has a long tradition in Asia because a clear and even complexion has been considered an ideal beauty in this continent for centuries. However, many common skin lightening ingredients are reported to be unsafe, cytotoxic, unstable, or ineffective at low concentrations. Phenylethyl resorcinol (PR), also known as 4-(1-phenylethyl)-1,3-benzenediol, is a relatively new and highly efficient skin-lightening agent [1, 2]. PR is a synthetic compound that is inspired from pinosylvin, a natural skin brightening compound that is found in pine. This antioxidant effectively influences pigmentation, thereby producing skin-lightening effects that do not result from cytotoxicity. A clinical study showed that 0.5% PR is more effective in skin lightening than 1.0% kojic acid [3]. However, the application of PR in cosmetic products remains limited by its instability and poor water solubility.

To overcome these limitations, the use of colloidal delivery system is proposed. Solid lipid nanoparticles (SLN) were developed at the beginning of the 1990s as an alternative colloidal lipidic system for controlled drug delivery [4]. The liquid lipid (oil) phase from regular O/W emulsion is replaced by a lipid mixture that remains solid at both room and body temperatures. The physical state of lipid particles plays a major role in increasing the stability of active compounds after their incorporation into lipid nanoparticles, especially solid state lipids. The liquid state of colloidal system allows the active ingredients to partition between

CONTACT W. Zhang zhwanp@126.com School of Perfume and Aroma Technology, Shanghai Institute of Technology, No.100, Haiquan Road,Fengxian district, Shanghai 201418, China.

the dispersed and continuous phases, thereby leading to the instability of the active ingredients in the continuous phase during storage [5]. Nanostructured lipid carriers (NLC) are new-generation SLNs whose oil phase is composed of solid and liquid lipids. In this case, the particles have more internal defects than those in SLN, and it favors accommodation of more guest molecules within the core region [6], thus facilitating the incorporation of an increased amount of drug, while preserving the physical stability of the nanocarriers [7]. NLC also remains in its solid state by controlling the liquid lipid content that is added to the formulation, therefore, the controlled drug release properties for NLC can be achieved. Widely and constantly studied, NLC is no longer an unfamiliar term for researchers. Although NLC loading with PR has been previously investigated [8], a delivery vehicle that combines NLC with liquid crystal (LC) structure for PR has yet to be explored.

LC shares the properties of conventional liquid and solid crystals [9]. In specific, LC may flow similar to liquid, but its molecules may be oriented in a crystal-like way. LC structure can be classified according to the conditions for the formation of molecular order. The lyotropic LC, which is used in this study, includes lamellar, hexagonal, and cubic structure and is an important part of the organized assemblies. These lyotropic liquid crystals exist not only in cell membranes but also in body organs, and most of all, the skin structure. This structural similarity can contribute to the skin compatibility of NLC and allow the PR which is loaded in the carriers to have an increased function on the skin. LC has already been applied in nanocarrier encapsulation technology in biology, pharmaceutics, and therapeutics, and has been proven propitious to drug loading and release [10–14]. Therefore, NLC with LC structure applying in cosmetics have an increased compatibility with the skin, can improve moisture retention, and may have effect on controlled drug release and penetration [15–20].

Combining the advantages of LC structure and NLC, we provide a new delivery vehicle for PR. Given its structural similarity to the intercellular lipids of the stratum corneum, which nature designed for the most effective control of the water retention and to maintain the healthiness of skin, large PR amounts are retained in the skin aside from water when the LC structure encapsulates PR. NLC can form a membrane structure on the skin to enhance this performance. Prolonged release and excellent stability can also be brought by NLC, which may improve the PR's effect even more.

2. Materials and methods

2.1. Materials

PR was provided by Symrise Co., Ltd. (Holzminden, Germany); triglyceride of caprylic-capricacid (GTCC) was received from Lubrizol (USA); behenyl alcohol was obtained from BASF Co., Ltd. (Ludwigshafen, Germany); cetearylglucoside was purchased from EVONIK-DEGUSSA Co., Ltd. (Essen, Germany). The water used throughout the experiments was deionized.

2.2. Preparation of NLC

NLC was prepared by melt and ultrasonication method [21]. Briefly, the lipid mixture (5.6%) was constituted of 1.0g behenyl alcohol, 0.5g GTCC and 0.5g PR, and melted at 85°C. Meanwhile, 0.8g cetearylglucoside and 47.2g water, forming the aqueous phase, were heated at 85°C as well. Then, pour the lipid mixture to the aqueous phase. The mixture was emulsified at 16,000 rpm for 3min, using an Ultra-Turrax® T-25 homogenizer (IKA®-Werke, Staufen,

Germany). Then, the coarse emulsion was ultra-sonicated by an ultrasonic processor (Cole-Parmer Instruments; Vernon Hills, Illinois, USA). The resulting suspensions were cooled down to room temperature under stirring condition.

2.3. Morphology analysis

The morphology of the samples was examined by transmission electron microscopy (TEM) (Tecnai G2 F30, FEI, USA) and scanning electron microscope (SEM), (Quanta 200 FEG, FEI, USA). Carbon filmed grid coating with the PR-NLC suspension was fixed with 1% osmic acid for 4 hours. After rinsing the grid with pure acetone for 3 times and 10 min each time, it was dried at 60°C in the oven for 48–72 hours. Then the samples were viewed under TEM and SEM and photographs were taken at suitable magnification.

2.4. Particle size and zeta potential analysis

Particle size (nm), polydispersity index (PDI), and zeta-potential (ZP, mV) of NLC were determined at 25°C by dynamic light scattering (DLS) using a Zetasizer Nano ZS (Malvern Instruments, Malvern, UK) equipped with a He-Ne laser operated at a wavelength of 633 nm. Measurements were performed at a fixed scattering angle of 90°. 1 mL of nanolipid carriers was placed into cuvettes of Beckman coulter after diluted 50 times with deionized water, and measurements were recorded. Analysis of particle size, PDI, and ZP was performed using manufacturer-supplied software that employed cumulant analysis. After performing measurements at least three times, we calculated means for each variable.

2.5. Storage stability

Stability of NLC was evaluated by measuring the average particle size and PDI. All samples were stored at room temperature for 9 weeks. The samples were dispersed in deionized water and characterized in terms of mean size and PDI. The average particle size was determined by cumulative analysis, and distribution was resolved using the Contin method [22].

2.6. High performance liquid chromatography (HPLC) measurement

The content of PR was analyzed by a high performance liquid chromatography (PE200, Perkin Elmer, USA). The HPLC system was equipped with an Inertsil ODS-2 column, coupled with a PESciex AP13000 MS-MS apparatus operating in the multiple reaction monitor mode. The mobile phase was a mixture of acetonitrile and water (50:50 v/v). The column was a C18 column (250 mm $\times$ 4.6 mm, 5 μm) (Aligent, USA).The flow rate was 1.0 mL/min, the detection wavelength was 290 nm (G1314A, JP11615541, UV detector, USA), and the column temperature was maintained at 35°C. Injected volume of the sample was 10 μL (Hu et al. 2006).

2.7. Drug encapsulation efficiency

Percent drug entrapment was determined and expressed as the ratio of experimentally measured amount of drug in dispersion and initial amount used for entrapment. First, a certain volume of NLC suspension was accurately taken, dissolved and diluted with anhydrous ethanol. Then, drug content in the resultant solution was determined by HPLC method described in item before, and the calculated drug amount was designated as W_{total}. To determine the unencapsulated drug the ultrafiltration centrifugal filter tubes with a molecular

weight cut-off of 30 kDa (Millipore, USA) [23] were used. Equal volume of PR-LC-NLC suspension was added into ultrafiltration centrifugal filter tubes and centrifuged at 12,000 rpm for 2 h at 4°C. The ultra-filtrate was diluted with anhydrous ethanol and drug content in the resultant solution was analyzed under the same HPLC condition. The amount of free drug was designated as W_{free}.

The drug encapsulation efficiency (E.E.) was calculated by the following equation:

$$E.E. = \frac{W_{total} - W_{free}}{W_{total}} \times 100\%$$

2.8. Lyophilization of PR-LC-NLC

Ideally, a freeze-dried nanoparticle should preserve the stability of nanoparticles while maintaining unaltered the initial nanoparticle parameters, such as hanging an adequate appearance, presenting a short reconstitution time, as long as being easily resuspended in water, and inducing no changes on particle size distribution of nanoparticles, while maintaining the encapsulated drug activity. Lyophilization of PR-LC-NLC was performed using sucrose (15% (w/v)) as cryoprotectant. The dispersion was pre-frozen for 12 h at −45°C and subsequently lyophilized at a temperature of −80°C for 24 h. The sample was put in a dryer and stored at room temperature afterwards.

2.9. Fourier transform infrared spectroscopy (FTIR) analysis

FTIR was performed using a Perkin Elmer system 2000 spectrophotometer to detectthe interaction between the drug and the lipid molecules. FTIR spectra of the samples were measured by a Fourier transform infrared spectrometer (AVATAR 360, Nicolet Instrument Corporation, USA). The spectra were employed at 400–4,000 cm^{-1} and a total of 32 scans were used.

2.10. Differential scanning calorimetry

Differential scanning calorimetry (DSC) analysis was performed using a DSC-Q200 differential scanning calorimeter (TA Instruments, USA). All formulation ingredients and freeze dried PR-LC-NLC were placed in aluminum pans, and the temperature was increased from 0°C to 150°C at a rate of 5°C/min under a dynamic nitrogen atmosphere with a flow rate of 50 mL/min. An empty pan was used as a reference.

2.11. Small angle X-ray scattering

Small Angle X-ray Scattering (SAXS) measurements were performed to study the LC structure of PR-LC-NLC by using a HMBG-SAX X-ray small angle system (Austria) with Ni-filtered Cu Kα radiation (0.154 nm) operating at 50 kV and 40 mA. All the measurements were made with 2 kW power, vacuum less than 10^{-3}MPa and a temperature of 25°C. The relative position of SAXS peaks on the scattering vector (q) axis was used to determine the structure of the liquid crystal phase.

2.12. Karl Fischer titration

A Karl Fischer Titration (ZSD–2, Anting Electronics, Shanghai, China) was used to determine micro amount of water content which presence in lamellar liquid crystalline. Lyophilized suspensions were measured. K·F reagent was calibrated by using the redistilled water. In this

measurement, water reacts with iodine and sulfur dioxide 10 μL (W′) of redistilled water was taken by using syringe and then injected into the titration cell where iodine and water react for coulometric titration, the number exhibited at the screen was A′, which represents the amount of Karl Fischer reagent that the titration consumed. And the water content was calculated by following equation:

$$F = \frac{\mathrm{W}'}{\mathrm{A}'}$$

$$\textit{Water content}\% = \mathrm{A} \times \frac{F}{W} \times 100\%$$

F: the amount of water that each milliliter of KF reagent consumed.
W: the weight of the sample (mg).
A: the amount of KF reagent that the sample consumed.

2.13. In vitro drug release

In vitro release studies were performed using the dialysis method. Generally, 2 mL of the dispersion was placed into a dialysis bag (molecular weight cut off 8000–14000; Viskase, USA), then placed into 40 ml of receiving phase constituted of phosphate buffer (pH 6.0) and ethanol (70:30, v/v). Samples of receiving phase were withdrawn at regular time intervals, and analyzed by HPLC method as described above. Fresh receiving mixture was added to maintain constant volume.

2.14. In vitro penetration

The penetration experiment was conducted in sink conditions. The artificial skin was selected from EMD Millipore Corporation (Billerica, U.S.A.). Vertical Franz diffusion cells (TP-6, Tianjin Xinzhou Science and Technology Co., Ltd., China) with a diffusion area of 1 cm^2 and a receptor compartment volume of 15 mL were used for permeation studies. The artificial skin was mounted on the Franz diffusion cell, with the shiny side contacting the donor compartment. An amount of 3mL of samples was applied on the skin surface in the donor compartment, and the receptor compartment of the cell was filled with phosphate buffer (pH 6.0) and ethanol (70:30, v/v). During the experiments, the solution in receptor side was maintained at 37 $\pm$ 0.5°C in order to ensure the surface skin temperature on the surface of the membrane and stirred at 800 rpm with Teflon-coated magnetic stirring bars. After application of the test formulation, 1mL of sample was analyzed at pre-determined time intervals (1, 2, 4, 6, 8, 10, 12, 24 h) and replaced by an equal volume of fresh receiving solution. After that, the skin retention was measured as well, by soaking the artificial skin in 20 mL of ethanol. The skin soaked in ethanol was then sonicated for 20 min using an Ultrasonic sonicator (KQ–250DE, Kun Shan, China). The resulting solution was then analyzed after filtrated to remove the macromolecule impurities.

2.15. Statistical analysis

All values were expressed as the mean value deviation. Statistical significance of differences was examined using one-way analysis of variance followed by a least significant difference post hoc test. The significance level was set at $p < 0.05$.

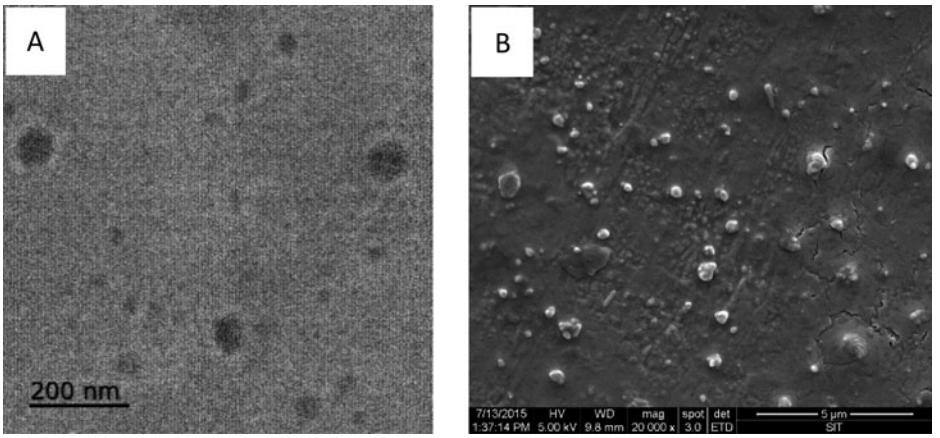

Figure 1. Sample morphology: A) TEM and B) SEM images of PR–LC–NLC.

3. Results and discussion

3.1. Morphological analysis

In order to provide information on the morphology of the PR-LC-NLC, TEM and SEM was used to take photos of the NLC formulation. As indicated in Fig. 1, the NLC particles were spherical with a homogenous shading and that the particles were approximately 100 nm in diameter and included some large objects that might be aggregation of particles that resulted from the pretreatment. Particle size measurements were performed to obtain precise information on size distribution.

3.2. Particle size and zeta potential analysis

Particle size and zeta potential are important physicochemical particle indexes that determine the physical stability and biopharmaceutical properties of the preparation [24]. The particle size and PDI of PR–LC–NLC were 153.9 ± 8.3 nm and 0.23 ± 0.01, respectively, with a negatively charged surface of −38.8 ± 0.6 mV. The diameter that was determined by DLS was larger than that observed by TEM and SEM (i.e., approximately 100 nm). Such divergence might be attributed to the fact that DLS might produce errors. The particles might be surrounded by a layer of water molecules during dynamic light scattering, which might result in a large particle size. In general, smaller particles (less than 200 nm) have a higher skin retention. Well-formulated systems should display a narrow particle size distribution in the submicron size range [25]. PDI indicates the width of the particle size distribution, which ranges from 0 to 1, and a PDI of < 0.3 is considered narrow size distribution [26]. A narrow PDI indicates the homogeneity of colloidal suspensions. The particles may disperse stably when the absolute value of zeta potential is above 30 mV because of the electric repulsion between particles [27].

3.3. Storage stability

During a nine-week storage at room temperature, the stability of the sample was detected by monitoring the particle size and PDI. NLC should improve the physical stability of the active ingredient loaded in it [28]. As shown in Fig. 2, the mean particle size did not significantly

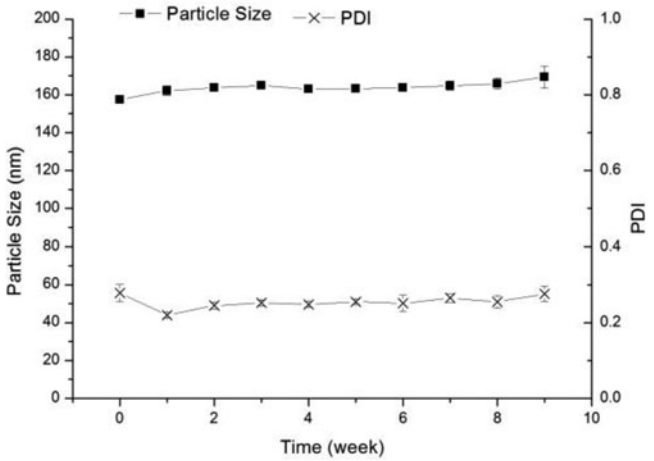

Figure 2. Mean particle size and PDI of PR–LC–NLC during the nine-week storage period.

change and ranged from 157.4 nm to 169.3 nm during the nine-week storage. According to Stoke's law, the particle radius is proportional to the flow settling velocity, which suggests that a smaller particle size leads to the slower settlement and higher stability of the particles. The sample had a favorable monodispersity because of the narrow size distribution indicated by the PDI values, which were all lower than 0.3 during the entire storage period. No creaming, flocculation, and coalescence were observed, suggesting that the prepared NLC had a favorable physical stability in the long-term storage. Therefore, the obtained formulation could be an excellent vehicle for PR when applied in products.

3.4. Drug encapsulation efficiency (E.E.)

Drug encapsulation efficiency is an important aspect of nanoparticles as ideal drug delivery carriers. The encapsulation efficiency of PR was 98.70%, as measured by HPLC. Such a high E.E. suggested that most of the PR was encapsulated in the NLC. This phenomenon could be explained by the liquid lipid in the lipid core of NLC, which could create a less-ordered crystalline in the solid lipid matrix, thereby increasing the PR content in the particles.

3.5. Fourier transform infrared spectroscopy (FTIR) analysis

FTIR was conducted to verify whether any interaction occurred between the lipid and the active ingredient, in this case, PR. Fig. 3 showed the FTIR spectra of pure PR, blank NLC, PR and blank NLC mixture (PR-mixture), and PR–LC–NLC. The FTIR spectrum of pure PR (Fig. 3A) revealed absorption bands at 3384.83 cm^{-1}, which could be attributed to hydrate O–H stretching. The intense bands at 3019.06 and 1602.26 cm^{-1} could be attributed to aromatic C–H and C = C stretching, respectively. The peaks at 699.98 and 546.79 cm^{-1} resulted from substituted benzene. These characteristic peaks of PR [29] were also present in the PR-mixture and pure PR. The FTIR spectra of blank NLC and PR–LC–NLC were almost the same. In the FTIR spectrum of PR–LC–NLC, the peaks that corresponded to PR (as indicated by the arrows in Fig. 3) could not be found or was weakened in the spectra of blank NLC, which indicated that PR was entrapped in the lipid matrix. Similar results were observed for other drugs [30–31] as well. This phenomenon could be explained by the drug-enriched core model for the

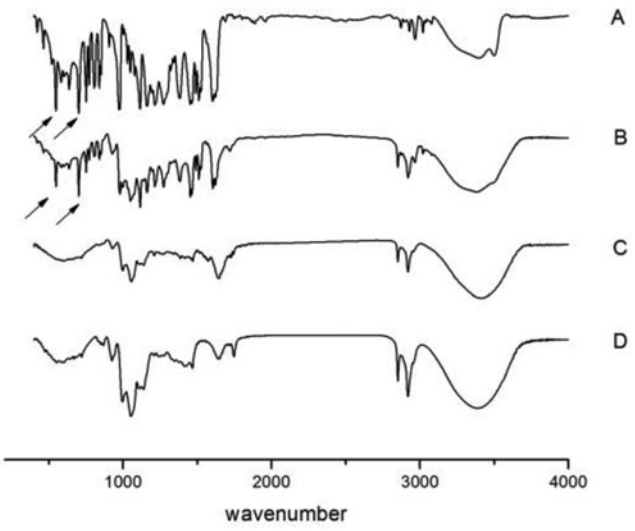

Figure 3. FTIR of the samples: (A) pure PR, (B) mixture of PR and blank NLC, (C) PR–LC–NLC, and (D) blank NLC.

incorporation of active compounds into SLN [32]. Similar to SLN, PR might start precipitating because of its high melting point as the core and other components (lipid and emulsifiers) might form a coating around the core.

3.6. Differential scanning calorimetry (DSC)

DSC is a thermo-analytical technique for studying crystallinity degree and polymorphic or thermal transitions that involve energy changes. Fig. 4 showed the DSC traces of (A) blank NLC, (B) PR–LC–NLC, and (C) pure behenyl alcohol. During heating, all samples showed an endotherm around 70°C. Two small peaks and a sharp peak were found in the DSC trace of pure behenyl alcohol (Fig. 4C), whereas blank NLC and PR–LC–NLC only had a relatively

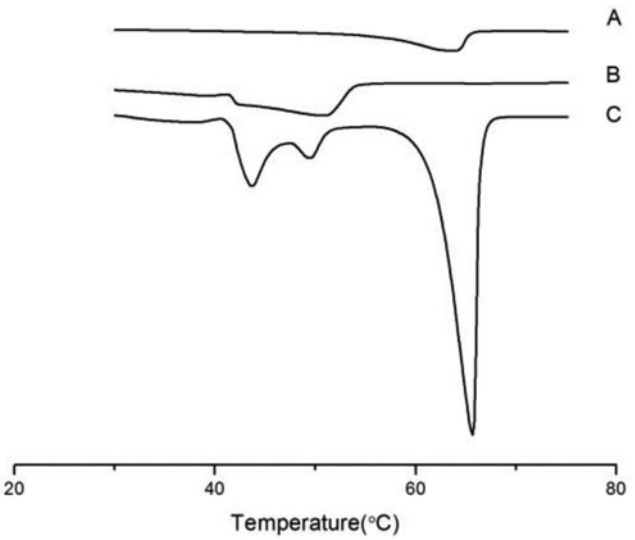

Figure 4. DSC traces of the samples: (A) blank NLC, (B) PR–LC–NLC, and (C) behenyl alcohol.

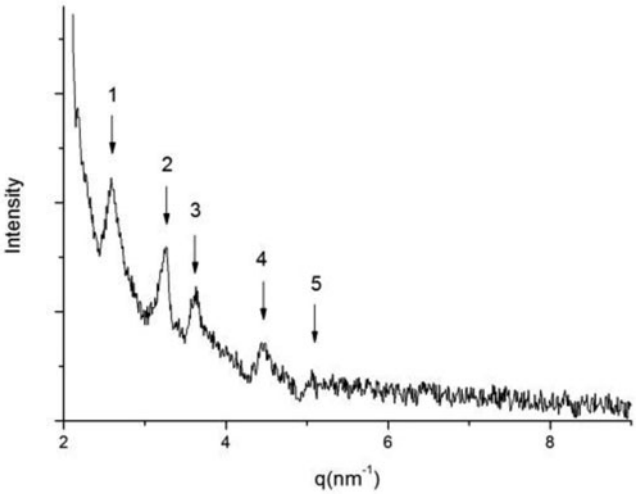

Figure 5. SAXS of PR-LC-NLC.

broad endotherm. This might be caused by the liquid crystal structure (so-called mesomorphic state) that the NLC possessed, instead, pure behenyl alcohol's crystalline is more aligned. Crystalline behenyl alcohol showed a sharp endothermic peak at 64.5°C, which corresponded to its melting point [33]. Conversely, given the colloidal size range of the lipid particles, a remarkably lower endothermic peak of lipid was observed in PR–LC–NLC and blank LC–NLC compared with that of pure behenyl alcohol. The shift in the melting point of NLC might be attributed to the interaction of solid and liquid lipids during the preparation process. A less-ordered crystal or amorphous lipid matrix could facilitate the encapsulation of greater amounts of drug [34].

3.7. Small angle X-ray scattering

The liquid crystalline of PR–LC–NLC was identified by SAXS. Fig. 5 showed that $q_1 : q_2 : q_3 : q_4 : q_5 = \sqrt{2} : \sqrt{3} : \sqrt{4} : \sqrt{6} : \sqrt{8}$. According to the literature [35], the LC of PR–LC–NLC was cubic, which was among the three structures of lyotropic LC. The cubic phase of LC is suitable for the design of nanostructured carriers and delivery systems by facilitating the encapsulation of active ingredients [36–37].

3.8. Karl Fischer titration

The liquid crystalline surrounding the droplets contains a multilayer structure of water[38]. Therefore, Karl Fischer titration was performed to determine the water content in the liquid crystalline. Aside from PR–NLC–LC dispersion, we prepared a regular emulsion with PR as the active ingredient (changing the solid lipid into liquid lipid — GTCC, while the total amount of the lipid remained the same as that in the original formulation) (PR–Emulsion) and used PR in NLC suspension without LC structure as control (changing behenyl alcohol and cetearylglucoside into pentaerythritol distearate and PEG-20 methyl glucose sesquistearate, respectively, while maintaining the quantity and the other parts of the formulation invariant of PR–LC–NLC) (PR–NLC). Table 1 showed that the water content of PR–LC–NLC was much higher than that of PR–Emulsion and PR–NLC without an LC structure. This result further proved that LC existed in our obtained suspension.

Table 1. Water content of PR–Emulsion, PR–NLC, and PR–LC–NLC.

	PR–Emulsion	PR–NLC	PR–LC–NLC
Water content (%)	2.3973	2.7394	4.4552

3.9. In vitro drug release

To achieve controlled release and obtain prolonged release information, the complete in vitro release profile was determined using dialysis. Fig. 6 showed the release of PR in the regular emulsion, NLC, and NLC with LC structure within 24 h. The PR release from the regular emulsion was superposable to that from the NLC. No significant differences were observed between PR–NLC and PR–LC–NLC. This finding might indicate that the LC structure did not influence in vitro drug release (needed further study) and that NLC could serve as an excellent vehicle for PR. In the PR–NLC formulation, the PR molecules were incorporated into the lipid matrix, and their diffusional mobility was decreased. In the case of PR-Emulsion, a release pattern was observed following an initial burst release of drug, which was then followed by a sustained release of drug at a constant rate. The PR that was encapsulated in the NLC displayed a release pattern that persistently increased along with a slower escalation rate but did not remain constant. This finding indicated that the NLC structure had a controlled release and a prolonged release effect. The initial burst release of NLC at 2 h might be attributed to a drug-enriched shell model for the incorporation of PR into the NLC system. A significant proportion of the active drug (80.38% and 74.89%) remained in the outer shell during supersaturation, which led to a short diffusion path from the drug to the release media [39]. Fig. 6 showed that the PR released from the NLC within 24 h was less than that from PR-Emulsion. This result suggested that instead of being diffused into the surrounding medium, more PR was retained in the skin because of the NLC structure.

3.10. In vitro penetration study

The in vitroskin penetration of PR–NLC and PR–LC–NLC was investigated through artificial skin using Franz diffusion. The PR-Emulsion was used as control. Fig. 7 showed the in vitro

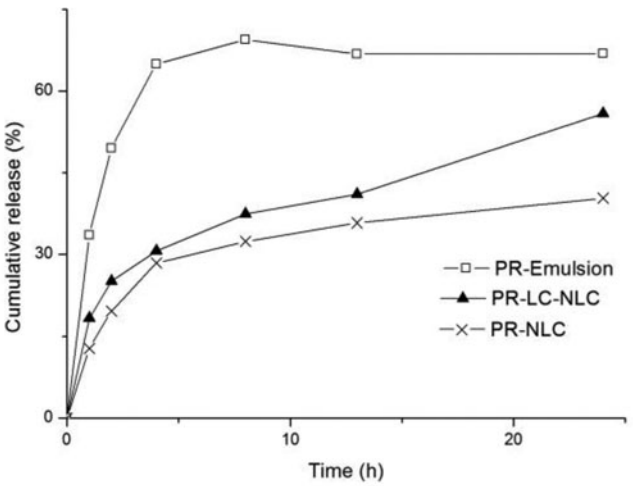

Figure 6. In vitro drug release of PR-Emulsion, PR–LC–NLC, and PR–NLC.

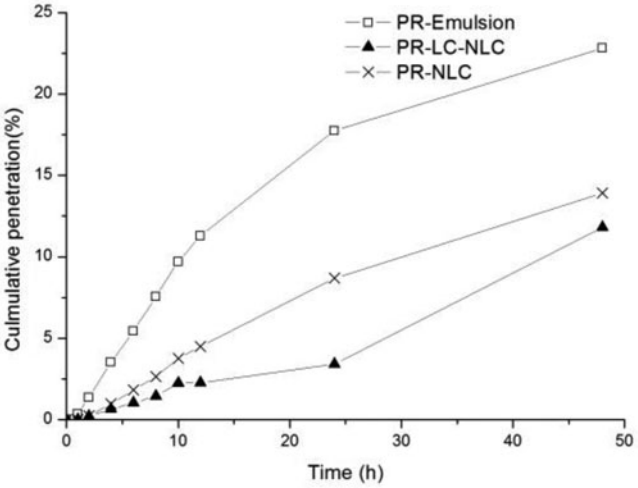

Figure 7. In vitro penetration of PR-Emulsion, PR–LC–NLC, and PR–NLC.

Table 2. Skin retention of PR-Emulsion, PR–NLC, and PR–LC–NLC.

	PR-Emulsion	PR–NLC	PR–LC–NLC
Skin retention(μg/mL)	388.84766	502.19852	653.9491

penetration of PR in the regular emulsion, NLC, and NLC with LC structure within 48 h. The PR penetration from PR-Emulsion was superposable to that from the NLCs with or without LC structure. By contrast, the penetration of PR–NLC was slightly superposable to that from PR-LC-NLC. Cosmetic actives should be localized in the skin without causing any systemic effects to avoid crossing the skin. As shown in Table 2, PR–LC–NLC retained more PR in the skin than PR-Emulsion and PR–NLC. The application of NLC to the skin led to the formation of films, to which the LC contributed because its structure was similar to the skin surface. The water of the suspension was evaporated, thereby leading to particle fusion and film formation. Given that PR was localized in this film, the penetration decreased, and the skin retention increased.

4. Conclusion

A promising delivery vehicle for PR was successfully manufactured. This vehicle combined the advantages of NLC and LC structure, including excellent stability, excellent water solubility, and high skin retention, thereby addressing the limitations of PR in its application in cosmetic products. PR–LC–NLC demonstrated a spherical morphology, high drug entrapment efficiency, and excellent long-term stability. The investigations on the drug–lipid interaction using FTIR spectroscopy confirmed the compatibility of PR with the carrier lipid. DSC analysis illustrated the thermo transition of the samples. The LC structure of the carrier was characterized using SAXS and Karl Fischer titration. A prolonged release profile of PR from PR–LC–NLC was obtained. When the PR was encapsulated into LC–NLC, the amount of PR that penetrated through the skin was reduced, whereas the accumulation of PR in the skin was increased. Therefore, NLC combined with LC structure has superior cosmetic applications over traditional emulsions.

References

[1] Schmaus, G., Vielhaber, G., Jacobs, K., & Franke, H. (2006). *J. Cosmet. Sci.*, *57*, 197–198.
[2] Vielhaber, G., Schmaus, G., & Jacobs, K. (2006). *IFSCC Mag.*, *9*, 2–9.
[3] Meyer, I., Knupfer, M., Joppe, H., Köhler, A., Hölscher, B., & Mansfeld, M. (2015). A cosmetic composition for lightening skin and/or hair, European Patent: EP2853254.
[4] Chen, X., Efrima, S., Reger, O., Wang, W., Niu, L., Sui, Z. M., Zhu, B. L., Yuan, X. B., & Yang, K. Z. (2001). *Sci. China Ser. B-Chem.*, *44*(5), 492–499.
[5] Teeranachaideekul, V., Müller, R. H., & Junyaprasert, V. B. (2007). *International Journal of Pharmaceutics*, *340*, 198–206.
[6] Luan, J., Zheng, F., Yang, X., Yu, A., & Zhai, G. (2015). *Colloids and Surfaces A: Physicochem. Eng. Aspects*, *466*, 154–159.
[7] Gainza, G., Bonafonte, D. C., Moreno, B., Aguirre, J. J., Gutierrez, F. B., Villullas, S., Pedraz, J. L., Igartua, M., & Hernandez, R. M. (2015). *Journal of Controlled Release*, *197*, 41–47.
[8] Fan, H. F., Liu, G. Q., Huang, Y. Q., Li, Y., & Xia, Q. (2014). *Applied Surface Science*, *288*, 193–200.
[9] Makai, M., Csányi, E., Németh, Z., Pálinkás, J., & Erõs, I. (2003). *Inter. J. Pharm.*, *256*, 95–107.
[10] Angelov, B., Angelova, A., Filippov, S., Drechsler, M., Stepanek, P., & Lesieur, S. (2014). *ACS Nano.*, *8*, 5216–5226.
[11] Angelova, A., Angelov, B., Lesieur, S., Mutafchieva, R., Ollivon, M., Bourgaux, C., Willumeit, R., & Couvreur, P. (2008). *J. Drug Deliv. Sci. Tech.*, *18*, 41–45.
[12] Angelov, B., Angelova, A., Filippov, S. K., Narayanan, T., Drechsler, M., Stepanek, P., Couvreur, P., & Lesieur, S. (2013). *J. Phys. Chem. Lett.*, *4*, 1959–1964.
[13] Angelov, B., Angelova, A., Filippov, S., Karlsson, G., Terrill, N., Lesieur, S., & Stepanek, P. (2011). *Soft Matter*, *7*, 9714–9720.
[14] Angelova, A., Angelov, B., Mutafchieva, R., & Lesieur, S. (2015). *J. Inorg. Organomet. Polym.*, *25*, 214–232.
[15] Guo, R., & Fu, Q. H. (2000). *Acta Chimical Sinica (in Chinese)*, *58*(10), 1196–1201.
[16] Vill, V., & Hashim, R. (2002). *Curr. Opin. Colloid In Sci.*, *7*, 395–409.
[17] Mu, J. H., Li, G. Z., Liao, G. Z., Huang, L., & Zhao, K. S. (2002). *Sci. China Ser. B-Chem.*, *45*(2), 184–190.
[18] Li, G. Z., Xiao, H. D., Li, Y., Mu, J. H., & Wang, L. W. (2001). *Chem. J. Chin. Uni. (in Chinese)*, *22*, 108–111.
[19] Boy, M., & Voss, H. (1998). *J. Mol. Catal. B-Enzym.*, *5*, 355–359.
[20] Sun, R. G., Zhang, J., & Wang, Y. C. (1998). *Sci. China Ser. B-Chem.*, *41*(1), 1–13.
[21] Esposito, E., Fantin, M., Marti, M., Drechsler, M., Paccamiccio, L., Mariani, P., Sivieri, E., Lain, F., Menegatti, E., Morari, M., & Cortesi, R. (2008). *Pharm. Res.*, *25*, 1521–1530.
[22] Jin, B.S., Lee, S.M., & Lee, K.H. (2006). *J. Kor. Ind. Eng. Chem.*, *17*, 138–143.
[23] Yue, P. F., Lu, X.Y., Zhang, Z. Z., Yuan, H. L., Zhu, W.F., Zheng, Q., & Yang, M. (2009). *AAPS Pharm. Sci. Tech.*, *10*, 376–383.
[24] Vandervoort, J., & Ludwig, A. (2002). *Int. J. Pharm.*, *238*, 77Y92.
[25] Uner, M. (2006). *Pharmazie*, *61*, 375–386.
[26] Das, S., Ng, W. K., & Tan, R. B. H. (2012). *European Journal of Pharmaceutical Sciences*, *47*, 139–151.
[27] Miao, J., Du, Y. Z., Yuan, H., Zhang, X. G., Li, Q., Rao, Y. F., Zhao, M. D., & Hu, F. Q. (2015). *J. Nanopart. Res.*, *17*, 109–21.
[28] Wissing, S. A., & Muller, R. H. (2002). *Journal of Controlled Release*, *81*, 225–233.
[29] Fan, H. F., Liu, G. Q., Huang, Y. Q., Li, Y., & Xia, Q. (2014). *Applied Surface Science*, *288*, 193–200.
[30] Bhalekar, M. R., Pokharkar, V., Madgulkar, A., & Patil, N. (2009). *AAPS Pharm. Sci. Tech.*, *10*, 289–296.
[31] Pople, P. V., & Singh, K. K. (2011). *European Journal of Pharmaceutics and Biopharmaceutics*, *79*, 82–94.
[32] Muller, R. H., Radtke, M., & Wissing, S. A. (2002). *Advanced Drug Delivery Reviews*, *54*, S131–S155.
[33] Kim, G. G., Poudel, B. K., Marasini, N., Lee, D. W., Hiep, T. T., Yang, K. Y., Kim, J. O., Yong, C. S., & Choi, H. G. (2013). *Drug Dev. Ind. Pharm.*, *39*(9), 1431–8.

[34] Lin, X., Li, X., Zheng, L., Yu, L., Zhang, Q., & Liu, W. (2007). *Colloids Surf. A Physicochem. Eng. Asp.*, *311*(1), 106–11.
[35] Angelov, B., Angelova, A., Drechsler, M., Garamus, V. M., Mutafchieva, R., & Lesieur, S. (2015). *Soft Matter*, *11*, 3686–3692.
[36] Angelov, B., Angelova, A., Garamus, V. M., Le Bas, G., Lesieur, S., Ollivon, M., Funari, S. S., Willumeit, R., & Couvreur, P. (2007). *J. Am. Chem. Soc.*, *129*, 13474–13479.
[37] Angelov, B., Angelova, A., Papahadjopoulos-Sternberg, B., Lesieur, S., Sadoc, J. F., Ollivon, M., & Couvreur, P. (2006). *J. Am. Chem. Soc.*, *128*, 5813–5817.
[38] Obeidat, W. M., Schwabe, K., Muller, R. H., & Keck, C. M. (2010). *European Journal of Pharmaceutics and Biopharmaceutics*, *76*, 56–67.
[39] Tran, T. H., Ramasamy, T., Truong, D. H., Choi, H. G., Yong, C. S., & Kim, J. O. (2014). *AAPS Pharm. Sci. Tech.*, *15*, 1509–1515.